Electrochromic Multilayer Films of Tunable Color by Combination of Copper or Iron Complex and Monolacunary Dawson-Type Polyoxometalate

Guanggang Gao,[†,‡] Lin Xu,[*,‡] Wenju Wang,[‡] Wenjia An,[‡] Yunfeng Qiu,[‡] Zhenqing Wang,[‡] and Enbo Wang[‡]

Department of Chemistry, Northeast Normal University, Changchun 130024, P. R. China, and Department of Chemistry, Jilin Normal University, Siping 136000, P. R. China

Received: December 9, 2004; In Final Form: February 21, 2005

Electrochromic multilayer films consisting of polyoxometalate (POM) cluster α-$K_{10}[P_2W_{17}O_{61}]\cdot 17H_2O$ (P_2W_{17}), copper(II) complex $[Cu^{II}(phen)_2](NO_3)_2$ (phen = 1,10-phenithroline), and iron complex $[Fe^{II}(phen)_3](ClO_4)_2$ were fabricated on silicon, quartz and ITO substrates by layer-by-layer self-assembly method. The multilayer films, $PSS/Cu^{II}(phen)_2/[(P_2W_{17}/Cu^{II}(phen)_2)]_n$ and $PSS/Fe^{II}(phen)_3/[(P_2W_{17}/Fe^{II}(phen)_3)]_n$ were characterized by UV−vis spectra, X-ray photoelectron spectra, cyclic voltammetry (CV), chronoamperometric (CA) and in-situ spectral electrochemical measurements. The interesting feature of the electrochromic film is its adjustable color by reduction of both transition metal complex and polyoxometalate at different potentials. The multilayer films also exhibit high optical contrast, suitable response time and low operation potential due to the presence of mono-lacunary-substituted polyoxometalate and transition metal complex. This is the first example that the color of electrochromic film can be adjustable, which gives valuable information for exploring new electrochromic materials with tunable colors.

Introduction

In recent years, polyoxometalates [abbreviated as POMs] attract increasing attention worldwide due to their intriguing structures and diverse properties,[1,2] such as catalytic activity for chemical transformation,[3] molecular conductivity,[4] magnetism,[5] luminescence, and photochromism and electrochromism.[6] One of the most important properties of these structurally well-defined polyoxometalate clusters is their ability to undergo reversible multiple electron transfer reactions. Because the reduction of polyoxometalate (for most of the POMs) exhibits blue color, the reduced POM is often called "heteropoly blue". Therefore, POMs can be used as electrochromic materials with blue color at the reduction state. Although a lot of electrochromic materials, such as transition metal oxides,[7−12] Prussian blue,[13] viologens,[14] conductive polymers,[15] lanthanide complexes,[16] transition metal complexes and metal phthalocyanines,[17,18] have received considerable attention, these materials have had little success because of the lifetime requirements, their cost-intensive production process, and their high price. For example, Prussian blue can be used as material for high contrast electrochromic film. However, when such film underwent double potential measurement to investigate its electrochromism, the absorbance decreased gradually with the potential cycles; this limited the practical application for electrochromic devices.[13] Furthermore, the films of transition metal oxide exhibit only slow response for achieving full contrast.[19] Although attempts have been made to modify these materials for improving performance, the exploration of POM-based electrochromic materials still remains a challenge. Tell and co-workers investigated the electrochromic properties of $H_3PW_{12}O_{40}\cdot 29H_2O$ and $H_3PMo_{12}O_{40}\cdot 29H_2O$ in 1978,[20,21] but these electrochromic cells have a disadvantage in that their bleach is slow when color intensified. Also, the cell's life is limited by an increase in cell impedance over time.[22]

Recently, Decher and co-workers developed an effective and convenient method for ultrathin film assembly, namely, the layer-by-layer (LBL) method, based on alternately electrostatic adsorption of oppositely charged species from dilute solutions. Some recent publications reported the successful fabrication of functional films containing both polyelectrolyte and polyoxometalate,[23,24] which not only confirms the feasibility of fabrication of multilayer films of polyoxometalate with polymers or large organic cations[25−29] but also brings a promising way to further develop such multilayer film materials. More recently, Kurth and co-workers reported the preparation of multilayer films containing POM cluster of $[Eu-(H_2O)P_5W_{30}O_{110}]^{12-}$ by layer-by-layer self-assembly method. These multilayer films of $[Eu-(H_2O)P_5W_{30}O_{110}]^{12-}$ displayed good electrochromism,[30] suggesting that more POMs with various structures should be investigated for developing applicable electrochromic materials. For example, Wells−Dawson type and those substituted POM anions can endure a reversible redox process in solution and multilayer films. However, the polyelectrolyte used as film matrix has no coloring activity, so that more bilayers containing POM are needed to obtain enough optical contrast; this obviously increases the response time due to the increased film thickness.[31] Therefore, it will be of practical importance to find some auxiliary electrochromic materials that not only interlink polyoxometalates but also display new color change.

In 1994, David Ingersoll et al. investigated the feasibility for $[Fe(phen)_3]^{3+}$ and polyoxometalate in different substrates by layer-by-layer method.[28] Two years later, Alexander Kuhn et al. explored the matching of $[Os(bpy)_3]^{2+}$ and $P_2Mo_{18}O_{62}^{6-}$ on electrode surfaces in the similar procedure.[27] Although these results suggest the feasibility to combine cationic metal complex with POM anion in film materials, the development of multi-

* Corresponding author. Tel.: +86-431-5269668. Fax: +86-431-5269668. E-mail address: linxu@nenu.edu.cn.
‡ Northeast Normal University.
† Jilin Normal University.

10.1021/jp044403n CCC: $30.25
Published on Web 04/12/2005

color electrochromic film is still limited due to the difficulty of searching for optimum matching.

In this paper, we find a rational combination of two kinds of electrochromic matrix, a POM anion α-$K_{10}[P_2W_{17}O_{61}]\cdot 17H_2O$ (P_2W_{17}) and a cationic metal complex $[Cu(phen)_2](NO_3)_2$ or $[Fe(phen)_3](ClO_4)_2$, incorporating them into the ultrathin multilayer films. Using the polyoxometalate and metal complex as electrochromic materials, the PSS/$Cu(phen)_2$/$[(P_2W_{17}/Cu(phen)_2)]_{30}$ or PSS/$Fe(phen)_3$/$[(P_2W_{17}/Fe(phen)_3)]_{30}$ film can display color change from light green, yellow, green to green blue, and orange red to deeper violet, respectively. These color changes are adjustable depending on the reduction extent of P_2W_{17}, by applying more negative potentials. Also, their performance of higher contrast, suitable response time and low operation potential should be promising to meet the requirement for developing flexible displays and electrochromic devices.

2. Experimental Section

2.1. Materials. α-$K_{10}[P_2W_{17}O_{61}]\cdot 17H_2O$ (P_2W_{17}), $[Cu^{II}(phen)_2](NO_3)_2$, and $[Fe^{II}(phen)_3]$ $(ClO_4)_2$ were prepared according to literature methods and identified by UV−vis absorption spectra, cyclic voltammetry, and elemental analysis.[32−35] Poly(stryenesulfonate) (MW 70 000) and (3-aminopropyl)-trimethoxysilane were purchased from Aldrich and used without further treatment. All other reagents were of AR grade. The deionized water was used in all experiments with a resistivity of 18 MΩ cm.

2.2. Preparation of the $[P_2W_{17}/Cu(phen)_2]_n$ and $[P_2W_{17}/Fe(phen)_3]_n$] Films. Silicon, quartz substrates, and ITO-coated glass were used for the film fabrication of self-assembly. The surface of silicon (1.0× 1.0 cm^2), quartz (1.0 × 2.0 cm^2) and ITO-coated glass (1.0 × 2.0 cm^2) were cleaned in an $H_2O/H_2O_2/NH_4OH$ (1:1:1) bath for 20 min and then washed by ultrasonic bath with large quantity of deionized water, followed the preparation process of multilayer films. First, a precursor film was deposited on a cleaned substrate by immersing the substrate alternately in (3-aminopropyl)trimethoxysilane, poly(styrenesulfonate) (containing 1 M NaCl; pH ∼ 4.0), and $[Cu(phen)_2]^{2+}$ (3×10^{-3} M) (or $[Fe(phen)_3]^{2+}$ (3×10^{-3} M)) solutions for 2 h, 20 min, and 10 min, respectively, followed by rinsing with deionized water and drying in a gentle nitrogen stream after each immersion. The substrate-supported precursor film was thus alternately dipped into the $[P_2W_{17}]$ (2×10^{-3} M) in HOAc−NaOAc buffer pH ∼ 3.5−3.7) and $[Cu(phen)_2]^{2+}$ (or $[Fe(phen)_3]^{2+}$) solutions for 10 min and rinsed with deionized water after each dipping. This process can be repeated until the desired number of bilayers of $[P_2W_{17}/Cu(phen)_2]$ or $[P_2W_{17}/Fe(phen)_3]$ is achieved, and all adsorption procedures were performed at room temperature. Such multilayer films is expressed here as $[P_2W_{17}/Cu(phen)_2]_n$ or $[P_2W_{17}/Fe(phen)_3]_n$.

2.3. Physical Measurements. UV−vis absorption spectra of quartz- and ITO-supported films were recorded on a 756CRT UV−visible spectraphotometer. XPS spectra were measured on a silicon wafer using an Escalab-MK II phtoelectronic spectrometer with ALK2 (1486.6 eV) The cyclic voltammetric and chronoamperometry measurements were carried out by using CHI 660 electrochemical workstation at ambient temperature (25 °C). The pH value measurements were performed on a Model-Df808 digital pH/ion meter. A buffer solution was composed of NaOAc, acetic acid, and NaOH solutions. The ITO electrode coated with the self-assembled films was used as the work electrode, with a platinum coil as the counter electrode and the Ag/AgCl (3M KCl) as the reference electrode. Spectroelectrochemical measurements of $[P_2W_{17}/Cu(phen)_2]_n$ or $[P_2W_{17}/Fe(phen)_3]_n$ film were performed by combining the in situ UV−vis spectrophotometer with the electrochemical analyzer.

3. Results and Discussion

3.1. Fabrication of the Electrochromic Multilayer Film. The spontaneous layer-by-layer self-assembly of the anionic $[P_2W_{17}O_{61}]^{10-}$ and the cationic $[Cu(phen)_2]^{2+}$ or $Fe(phen)_3^{2+}$ onto the positive surface of the substrate modified with a precursor film depends basically on the electrostatic attraction between the oppositely charged species. Therefore, compared with the Wells−Dawson type polyoxometalate $[P_2W_{18}O_{62}]^{6-}$, $[P_2W_{17}O_{61}]^{10-}$ is more suitable to the layer-by-layer self-assembly method due to the increased four additional charge that plays an important role in strengthening the electrostatic adsorption. The key to a regular multilayer buildup is the reversal of the surface charge in each adsorbed layer. The precursor film is essential for gaining a more homogeneous, positive charge distribution on the surface of the substrate and for being of benefit to the subsequent reproducible deposition.[36] It was also necessary to rinse the films with deionized water after each adsorption step. With the above-mentioned fabrication procedure, highly reproducible films with controlled thickness can be obtained.

In PSS/$Cu(phen)_2$/$[(P_2W_{17}/Cu(phen)_2)]_{30}$ film, $[Cu(phen)_2]^{2+}$ was first reduced to $[Cu(phen)_2]^{+}$, followed a color change from light green to yellow in lower negative potential. When the more negative potential was operated, the P_2W_{17} was reduced to become a blue color. Dark blue color could appear with the more negative potentials, and the whole film displayed color change as light green, yellow, green, and green blue, which not only realized the multicolor changing but also made the color change tunable by different potentials. Further, the PSS/$Fe(phen)_3$/$[(P_2W_{17}/Fe(phen)_3)]_{30}$ film can also display color change from orange red to dark violet due to the mixed color of the reduced P_2W_{17} at more negative potential, which confirmed again the feasibility to use POM as a substrate of tunable color and to realize the multicolor change.

3.2. UV−Vis Spectra and X-ray Photoelectron Spectra. UV−vis spectroscopy was used in the present work to monitor the layer-by-layer assembling process of $[P_2W_{17}/Cu(phen)_2]_n$ and $[P_2W_{17}/Fe(phen)_3]_n$ films. Figure 1b shows the UV−vis absorption spectra of $[P_2W_{17}/Cu(phen)_2]_n$ multilayers (with $n = 0-30$) assembled on a precursor-coated quartz substrate (on both sides). The inset in Figure 1b displays the plots of the absorbance of quartz-supported $[P_2W_{17}/Cu(phen)_2]_{30}$ multilayer films at wavelength 208, 228, 278, and 301 nm as a function of the number of $[P_2W_{17}/Cu(phen)_2]$ bilayers. It can be seen in Figure 1b that all the films exhibit the characteristic absorption of the $[Cu(phen)_2]^{2+}$ cation in the UV region at 228, 278, and 301 nm as compared to the $[Cu(phen)_2]^{2+}$ solution (Figure 1a), confirming the incorporation of $[Cu(phen)_2]^{2+}$ into the composite films. The first absorption band at ca. 208 nm results from a overlap of both $[Cu(phen)_2]^{2+}$ (at 203 nm) and P_2W_{17} (at 209 nm) bands. A slight red shift appears for the bands at 228, 278, and 301 nm, as compared to that of $[Cu(phen)_2]^{2+}$ solution (Figure 1a; at 225, 275, and 295 nm). This maybe relates to the electrostatic interaction between the P_2W_{17} and $[Cu(phen)_2]^{2+}$. The absorption band at 225 nm for the precursor film is a feature of benzene chromophores in PSS and overlaped after additional bilayers. For $[P_2W_{17}/Fe(phen)_3]_n$ films, we obtained results similar to those of $[P_2W_{17}/Cu(phen)_2]_n$ in the incorporation of $[Fe(phen)_3]^{2+}$ and P_2W_{17} into the composite films (Figure 1c). There is only a little difference for $[P_2W_{17}/Fe(phen)_3]_n$ films, that the

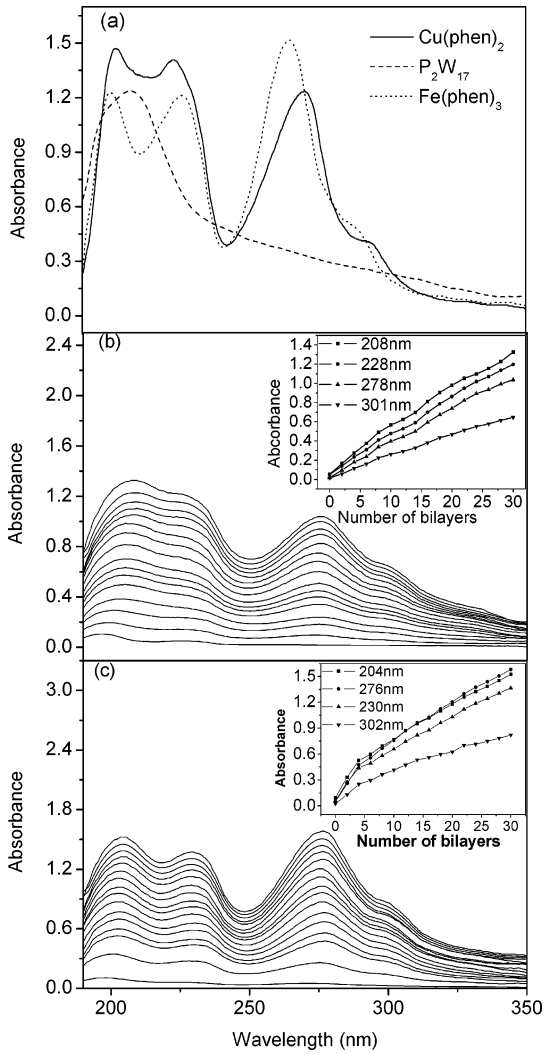

Figure 1. (a) UV spectra of 10^{-5} mol/L P_2W_{17}, $[Cu^{II}(phen)_2]^{2+}$, and $[Fe^{II}(phen)_3]^{2+}$ solutions. (b) UV spectra of $[P_2W_{17}/[Cu^{II}(phen)_2]]_n$ film with $n = 0-30$ for the precursor film-modified quartz substrate (on both sides). Bottom to top: $n = 0$, 2, 4, 6, 8, 10, 12, 14, 16, 18, 20, 22, 24, 26, 28, and 30, respectively. Inset: plots of the absorbance values at 208, 278, 228, and 301 nm. (c) UV spectra of $[P_2W_{17}/[Fe^{II}(phen)_3]]_n$ film with $n = 0-30$. Inset: plots of the absorbance values for quartz-supported $[P_2W_{17}/[Fe^{II}(phen)_3]]_n$ multilayer films with $n = 0-30$ at 204, 276, 230, and 302 nm.

red shift from 290 to 302 nm is larger than that for $[P_2W_{17}/Cu(phen)_2]_n$ films, indicating the presence of different interaction between their metal complex and polyoxometalate.

To identify the elemental composition of the multilayer films, we measured the X-ray photoelectron spectra (XPS) of the $[P_2W_{17}/Cu(phen)_2]_4$ and $[P_2W_{17}/Fe(phen)_3]_4$ film on silicon substrates. Although the XPS measurement gives only semi-quantitative elemental composition, the presence of C, O, N, P, Cu, Fe, and W elements in the film are confirmed, and the expected molar ratio of 2:17 for P to W, 1:4 for Cu to N and 1:6 for Fe to N are also approximately established. The XPS of $[P_2W_{17}/Cu(phen)_2]_4$ and $[P_2W_{17}/Fe(phen)_3]_4$ films are shown in Figure 2. The XPS data suggest that we indeed incorporate both anionic P_2W_{17} and cationic $[Cu(phen)_2]^{2+}$ and $Fe(phen)_3^{2+}$ into the multilayer films. Furthermore, the W4f7/2 peaks (34.9 and 34.6 eV for $[P_2W_{17}/Cu(phen)_2]_3$ and $[P_2W_{17}/Fe(phen)_3]_3$ film, respectively) in the XPS measurement reflect that a little difference of chemical environment for P_2W_{17} in these films, which is in agreement to the UV−vis spectra results.

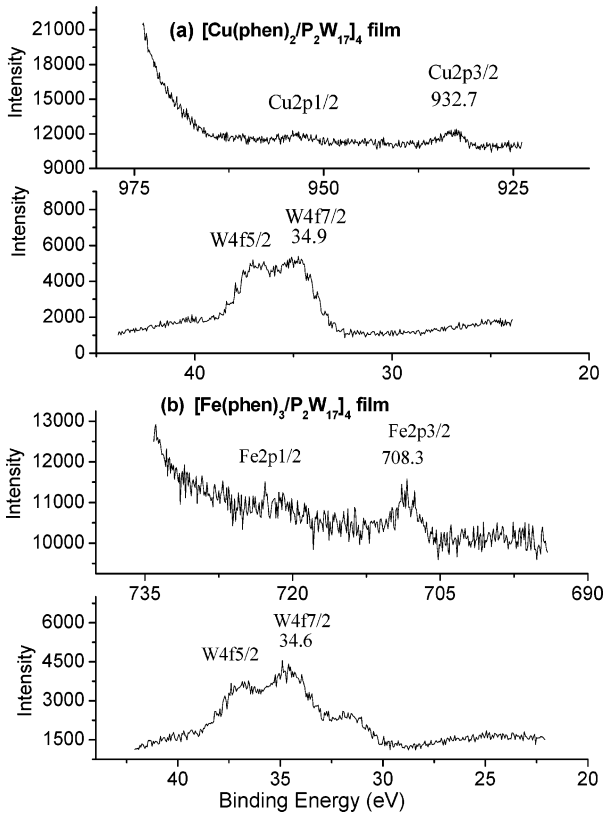

Figure 2. XPS spectra in the W (4f), Cu (2p), and Fe (2p) regions for (a) $[P_2W_{17}/[Cu^{II}(phen)_2]]_4$ and (b) $[P_2W_{17}/[Cu^{II}(phen)_2]]_4$ films.

3.3. Cyclic Voltammetry Spectra for $[P_2W_{17}/Cu(phen)_2]_n$ and $[P_2W_{17}/Fe(phen)_3]_n$ Films. Cyclic voltammetry (CV) of an aqueous 1 mM P_2W_{17} solution (in 0.2 M HOAc−NaOAc buffer at pH = 3.5), using a bare ITO-coated glass electrode (immersion area 1.0 × 0.5 cm^2), shows three clear potential peaks, $A_1 = -0.0813$ V, $A_2 = -0.3135$ V, and $A_3 = -0.5830$ V, during the anodic sweep and three potential peaks, $C_1 = -0.2629$ V, $C_2 = -0.4986$ V, and $C_3 = -0.7469$ V, during the cathodic sweep (Figure 3a). A_1, A_2, and A_3 are the anodic counterparts of C_1, C_2, and C_3, and the peak pairs C_1/A_1, C_2/A_2, and C_3/A_3 corresponds to the $2e^-/2H^+$ redox process.[32,33] However, the peak values are somewhat different from those reported in the literature, because the authors employed different electrolyte and experimental parameters.

Cyclic voltammograms of the $[P_2W_{17}/Cu(phen)_2]_{30}$-modified ITO electrode (immersion area 1.0 × 1.1 cm^2) in HOAc−NaOAc buffer solution with pH = 3.5, using a platinum coil as the counter electrode and Ag/AgCl/KCl (3 mol/L) as reference electrode, displays four anodic peaks, −0.0026 (c1), −0.3553, −0.5320, and −0.7804 V during the cathodic sweep and four cathodic peaks −0.2274 (a1), −0.5048, −0.6226, and −0.8707 V during the anodic sweep (Figure 2b). The first pair of peaks is due to the redox process for $[Cu(phen)_2]^{2+}$ in the film. Compared to P_2W_{17} solution, the other three pairs of peaks shift more negatively. It can be seen from Figure 3b (dot line) that cyclic voltammograms of the $[P_2W_{17}/Fe(phen)_3]_{30}$ film exhibit three pairs of peaks, which shift negatively larger than the corresponding peaks for P_2W_{17} solution. The $[Fe(phen)_3]^{2+}$ is relatively stable when compared to the oxidized state $[Fe(phen)_3]^{3+}$. Therefore, the redox process between $[Fe(phen)_3]^{3+}$ and $[Fe(phen)_3]^{2+}$ cannot be observed here for the $[P_2W_{17}/Fe(phen)_3]_{30}$ film.[34] Both the negative shifts for these films indicate the existence of different interactions between the two kinds of metal complexes and P_2W_{17}, which is in agreement with the

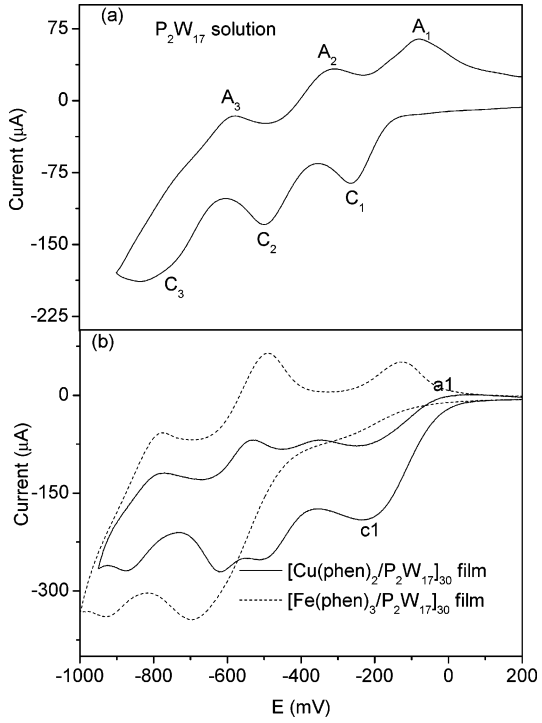

Figure 3. (a) Cyclic voltammograms of 1 mM P_2W_{17} in solution (ITO-coated glass as working electrode). (b) $[P_2W_{17}/[Cu^{II}(phen)_2]]_{30}$-modified (solid line) and $[P_2W_{17}/[Fe^{II}(phen)_2]]_{30}$-modified (dot line) ITO electrodes in HAc−NaAc buffer solution. (Platinum coil as the counter electrode and Ag/AgCl/KCl (3 mol/L) as the reference electrode with scan rate = 20 mV/s).

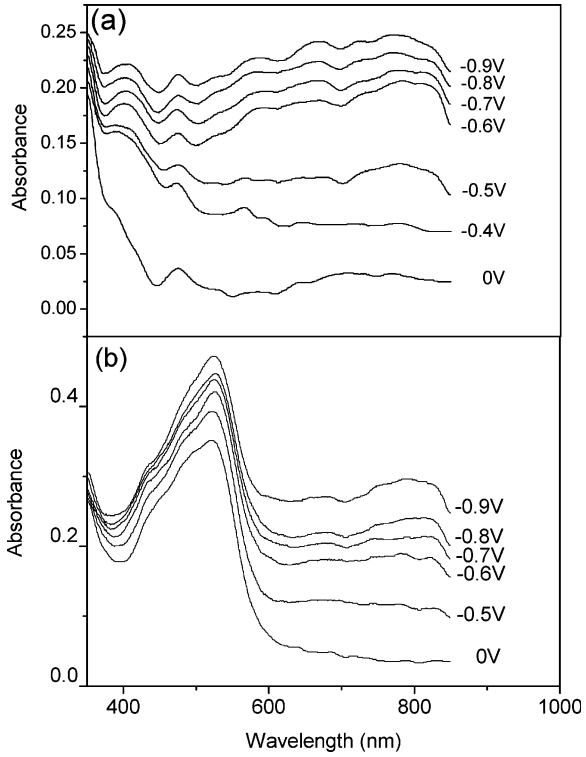

Figure 4. Visible spectra of (a) $[P_2W_{17}/[Cu^{II}(phen)_2]]_{30}$-modified and (b) $[P_2W_{17}/[Fe^{II}(phen)_3]]_{30}$-modified ITO glass electrodes at different potentials.

results of UV−vis spectra and XPS spectra. The CV curve of P_2W_{17} in solution and in multilayer films demonstrates that the electrochemical property of P_2W_{17} is fully maintained in the film, except a slightly negative shift of redox peak.

3.4. Electrochromism Investigation. The color change of P_2W_{17} in 0.2 M HOAc−NaOAc buffer solution during the CV measurement originates in the presence of an intervalence charge-transfer band (W^V-O-W^{VI} or $W^{VI}-O-W^V$), which is influenced by an applied potential and hence manifests itself in electrochromism. For the multilayer film $[P_2W_{17}/Cu(phen)_2]_{30}$, the $[Cu(phen)_2]^{2+}$ is reduced to display yellow color first at ca. −230 mV. When more negative potentials are applied, this yellow color is then mixed with the blue color resulting from the further reduced P_2W_{17}; this film thus displays light green, yellow, green to green-blue color under different potentials (Figure 4a). Similarly, as for the film $[P_2W_{17}/Fe(phen)_3]_{30}$, $[Fe(phen)_3]^{2+}$ displays orange red and is very stable in such conditions. When more negative potentials are applied, the P_2W_{17} is reduced to different extent blue colors, mixed with orange red color of $[Fe(phen)_3]^{2+}$ cation, to display orange red, light violet, and deeper violet, respectively (Figure 4b). The above results confirm the feasibility to successfully fabricate multicolor films by combining transition metal complex with polyoxometalates.

The response times of the film were investigated by the double-potential experiments as well as the absorbance measurement. The coloration and bleaching time is 6.6 and 6.5 s for 90% ΔA (difference between maximum and minimum absorbance), respectively, and the absorbance at about 650 nm increases 0.24 unit for $[P_2W_{17}/Cu(phen)_2]_{30}$ film. At the same time, the electrochromic reversibility of the film was evaluated by performing repetitive double potential steps from −900 to 500 mV (Figure 5a). The response times for both coloration and bleaching as well as the absorbance of the electrochromic film do not change noticeably even after 200 cycles, except for a little decrease of maximum absorbance (9%) (Figure 5a, dotted line), which demonstrates a little loss in the self-assembled films during double potential cycles. Compared to $[P_2W_{17}/Cu(phen)_2]_{30}$, the $[P_2W_{17}/Fe(phen)_3]_{30}$ film shows higher stability after 200 cycles repetitive double potential steps, with only the maximum absorbance decreasing 4% (Figure 5b dot line).

However, the coloring and bleaching time increases a little more as 7.4 and 7.0 s, respectively, at 650 nm for 90% ΔA. Obviously, the response times of the two kinds of film are slightly different because of the incorporation of different transition metal complexes into the multilayer films. These results demonstrate that P_2W_{17}, $[Cu(phen)_2]^{2+}$, and $[Fe(phen)_3]^{2+}$ are possible promising electrochromic materials for multicolor or color tunable devices. In addition, more bilayers of film can be increased to compensate for the weak optical contrast, because the layer-by-layer method is able to control the number of bilayers.[30]

3.5. Thermal Stability of the Films on Quarts Substrate. Because the UV−vis spectra of these films have hardly changed during all experiments, it is evident that these multilayer films are robust and stable at ambient temperature. To examine the thermal stability of these films, UV−vis spectra were measured after heating (or cooling) the film for 30 min at different temperature. The UV−vis absorption spectra for the quartz-coated $[P_2W_{17}/Cu(phen)_2]_{30}$ and $[P_2W_{17}/Fe(phen)_3]_{30}$ after heating (or cooling) are almost the same as that without heating (or cooling), and the characteristic bands of P_2W_{17}, $[Cu(phen)_2]^{2+}$, and $[Fe(phen)_3]^{2+}$ still remain. Especially, even the film sample is heated to 150 °C, the absorbances of the two characteristic bands (208 and 278 nm for $[P_2W_{17}/Cu(phen)_2]_{30}$ and 204 and 276 nm for $[P_2W_{17}/Fe(phen)_3]_{30}$) still are the same as those without heating or cooling (Figure 6), suggesting that such films have a considerable thermal stability.

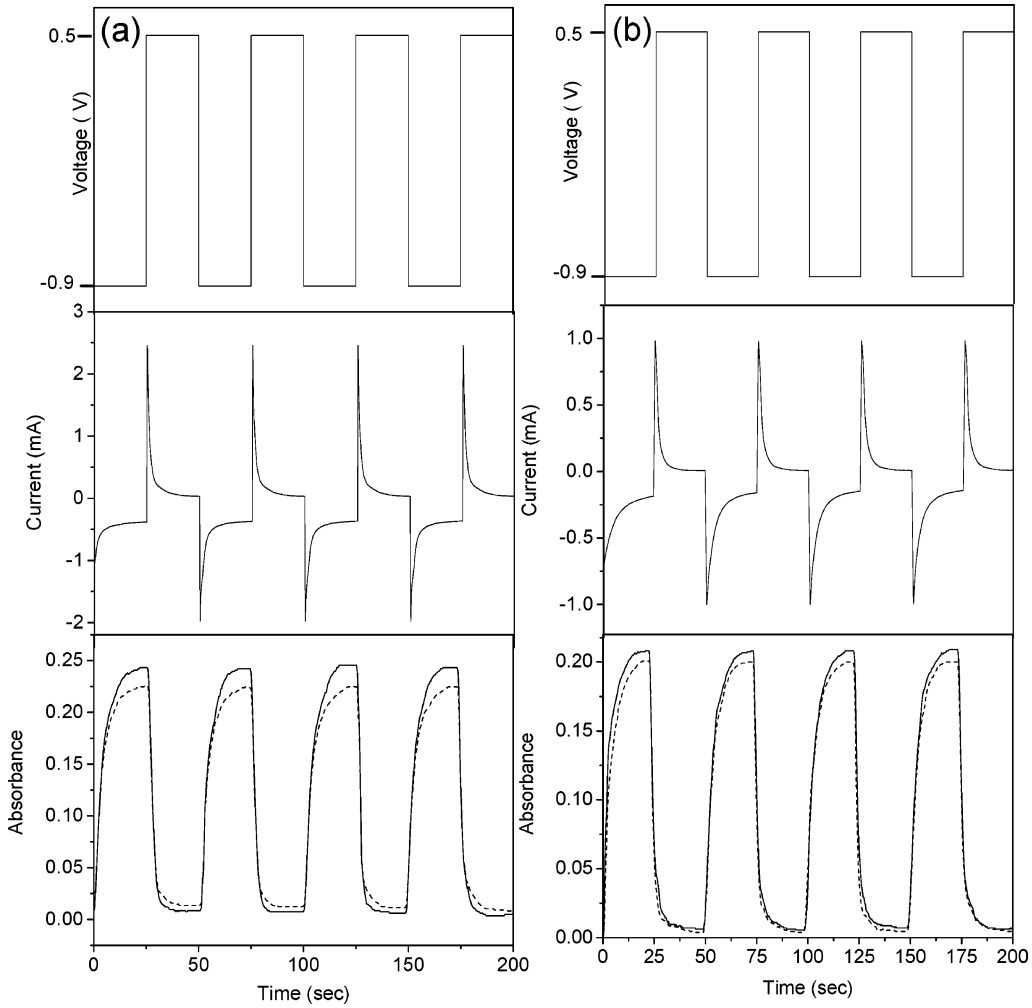

Figure 5. Potential, current, and absorbance at 650 nm of (a) $[P_2W_{17}/[Cu^{II}(phen)_2]]_{30}$-modified and (b) $[P_2W_{17}/[Fe^{II}(phen)_3]]_{30}$-modified ITO during subsequent double-potential steps (−900 to +500 mV).

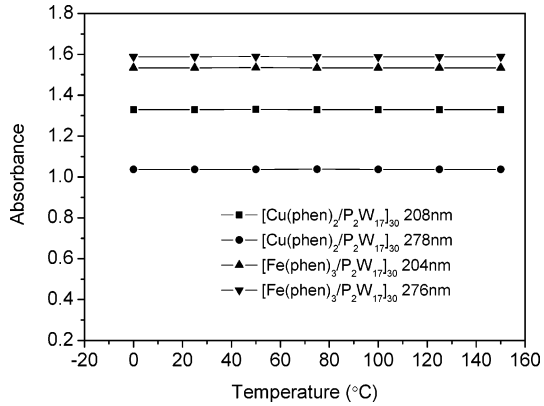

Figure 6. Temperature dependence of absorbance at characteristic band for the multilayer films.

4. Conclusions

New polyoxometalate-based electrochromic films of $[P_2W_{17}/Cu(phen)_2]_{30}$ and $[P_2W_{17}/Fe(phen)_3]_{30}$ were successfully fabricated by the layer-by-layer self-assembly method. The film materials consisting of both transition metal complex and P_2W_{17} show well electrochromism with suitable response time, low operation potential, good reversibility and thermal stability, suggesting that these materials may become promising candidates for the application of electrochromic materials. Moreover, the two kinds of films are of multicolor and color tunable electrochromic films, which not only confirm the feasibility for fabricating multicolor films based on both transition metal complex and polyoxometalates but also open a new route to develop polyoxometalate-based electrochromic materials.

Acknowledgment. We are thankful for the financial supports from the National Natural Science Foundation of China (Grant No. 20371010), the State Key Laboratory for Structural Chemistry of Unstable and Stable Species in Peking University (No. 03-12), and the Natural Science Foundation of Jilin Technology Office of China (No. 20030512-1).

References and Notes

(1) Pope, M. T.; Müller, A. *Polyoxometalates*: *From Platonic Solid to Anti-retroviral Activity*; Kluwer Academic Publishers: Dordrecht, The Netherlands, 1994.

(2) Hill, C. L. *Chem. Rev.* **1998**, *98*, 1.

(3) Branytska, O. V.; Neumann, R. *J. Org. Chem.* **2003**, *68*, 9510−9512 (Technical Note).

(4) Coronado, E.; Galán-Mascarós, J. R.; Giménez-Saiz, C.; Gómez-García, C. J.; Martínez-Ferrero, E.; Almeida, M.; Lopes, E. B. *Adv. Mater.* **2004**, *16*, 324−327.

(5) Coronado, E.; Clemente-León, M.; Galán-Mascarós, J. R.; Giménez-Saiz, C.; Gómez-García, C. J.; Martínez-Ferrero, E. *J. Chem. Soc., Dalton Trans.* **2000**, *21*, 3955−3961.

(6) Yamase, T. *Mol. Eng.* **1993**, *3*, 241.

(7) Monteiro, A.; Costa, M. F.; Almeida, B.; Teixeira, V.; Gago, J.; Roman, E. *Vacuum* **2002**, *64*, 287.

(8) Fang, G.; Yao, K.; Liu, Z. *Thin Solid Films* **2001**, *394*, 64.

(9) Antonaia, A.; Santoro, M. C.; Fameli, G.; Polichetti, T. *Thin Solid Films* **2003**, *426*, 281.
(10) Gesheva, K.; Szekeres, A.; Ivanova, T. *Solar Energy Mater. Solar Cells* **2003**, *76*, 563.
(11) Rosario, A. V.; Pereira, E. C. *Solar Energy Mater. Solar Cells* **2002**, *71*, 41.
(12) Ristova, M.; Velevska, J.; Ristov, M. *Solar Energy Mater. Solar Cells* **2002**, *71*, 219.
(13) DeLongchamp, D. M.; Hammond, P. T. *Adv. Funct. Mater.* **2004**, *14*, 224.
(14) Monk, P. M. S. *The Viologens: Physicochemical Properties, Synthesis and Applications of 4,4′-Bipyridine*; Wiley: Chichester, U.K., 1998.
(15) Groenendaal, L.; Jonas, F.; Freitag, D.; Pielartzik, H.; Reynolds, J. R. *Adv. Mater.* **2000**, *12*, 481.
(16) Notten, P. H. L. Curr. Opin. *Solid State Mater Sci.* **1999**, *4*, 5.
(17) McDonagh, A. M.; Bayly, S. R.; Riley, D. J.; Ward, M. D.; McCleverty, J. A.; Cowin, M. A.; Morgan, C. N.; Varrazza, R.; Penty, R. V.; White, I. H. *Chem. Mater.* **2000**, *12*, 2523.
(18) Tombach, N.; Hild, O.; Schlettwein, D.; Wohrle, D. *J. Mater. Chem.* **2002**, *12*, 879.
(19) Heuer, H. W.; Wehrmann, R.; Kirchmeyer, S. *Adv. Funct. Mater.* **2002**, *12*, 89.
(20) Tell, B.; Wudl, F. *J. Appl. Phys.* **1979**, *50*, 5944.
(21) Tell, B.; Waguer, S. *Appl. Phys. Lett.* **1978**, *33*, 873.
(22) Yamase, T. *Chem. Rev.* **1998**, *98*, 307.
(23) Jiang, M.; Wang, E.; Xu, L.; Kang, Z.; Lian, S. *J. Solid State Chem.* **2004**, *177*, 1776−1779.
(24) Ma, H. Y.; Peng, J.; Han, Z.; Feng, Y. H.; Wang, E. *Thin Solid Films* **2004**, *446*, 161−166.
(25) Cheng, L.; Pacey, G. E.; Cox, J. A. *Electrochim. Acta* **2001**, *46*, 4223−4228.
(26) Kulesza, P. J.; Chojak, M.; Miecznikowski, K.; Lewera, A.; Malik, M. A.; Kuhn, A. *Electrochem. Commun.* **2002**, *4*, 510−515.
(27) Kuhn, A.; Anson, F. C. *Langmuir* **1996**, *12*, 5481−5488.
(28) Ingersoll, D.; Kvlesza, P. J.; Faulkner, L. R. *J. Electrochem. Soc.* **1994**, *141*, 140.
(29) Moriguchi, I.; Fendler, J. H. *Chem. Mater.* **1998**, *10*, 2205−2211.
(30) Liu, S.; Kurth, D. G.; Möhwald, H.; Volkmer, D. *Adv. Mater.* **2002**, *14*, 225.
(31) Gao, G.; Xu, L.; Wang, W.; An, W.; Qiu, Y. *J. Mater. Chem.* **2004**, *14*, 2024−2029.
(32) McCormac, T.; Fabre, B.; Bidan, G. *J. Electroanal. Chem.* **1997**, *425*, 49−54.
(33) Keita, B.; Girard, F.; Nadjo, L.; Contant, R.; Canny, J.; Richet, M. *J. Electroanal. Chem.* **1996**, *478*, 76−82.
(34) Morehouse, S. M.; Suliman, H.; Haff, J.; Nguyen, D. *Inorg. Chim. Acta* **2000**, *297*, 411−416.
(35) Chen, S.-M. *J. Electroanal. Chem.* **1998**, *457*, 23−30.
(36) Ichinose, I.; Tagawa, H.; Mizuki, S.; Lvov, Y.; Kunitake, T. *Langmuir* **1998**, *14*, 187.